

PREPRINT/11/72

2001/156/923

545146  
P36

**Semiclassical Models for Virtual Antiparticle Pairs,  
the Unit of Charge  $e$ , and the QCD Coupling  $\alpha_s$**

David Batchelor

NASA's Goddard Space Flight Center

Greenbelt, MD 20771

E-mail address: david.batchelor@gsfc.nasa.gov

Accepted for publication in *Foundations of Physics*, 2002

New semiclassical models of virtual antiparticle pairs are used to compute the pair lifetimes, and good agreement with the Heisenberg lifetimes from quantum field theory (QFT) is found. The modeling method applies to both the electromagnetic and color forces. Evaluation of the action integral of potential field fluctuation for each interaction potential yields  $\approx \hbar/2$  for both electromagnetic and color fluctuations, in agreement with QFT. Thus each model is a quantized semiclassical representation for such virtual antiparticle pairs, to good approximation. When the results of the new models and QFT are combined, formulae for  $e$  and  $\alpha_s(q)$  are derived in terms of only  $\hbar$  and  $c$

**Abstract**

New semiclassical models of virtual antiparticle pairs are used to compute the pair lifetimes, and good agreement with the Heisenberg lifetimes from quantum field theory (QFT) is found. The modeling method applies to both the electromagnetic and color forces. Evaluation of the action integral of potential field fluctuation for each interaction potential yields  $\approx \hbar/2$  for both electromagnetic and color fluctuations, in agreement with QFT. Thus each model is a quantized semiclassical representation for such virtual antiparticle pairs, to good approximation. When the results of the new models and QFT are combined, formulae for  $e$  and  $\alpha_s(q)$  are derived in terms of only  $\hbar$  and  $c$ .

## 1. INTRODUCTION

Semiclassical methods have limitations and depend upon classical dynamics, which is rigorously valid only for large quantum numbers. Nevertheless, the Bohr model and a Bohr-Sommerfeld-type model of meson spectra developed by Brau<sup>(1)</sup> exhibit impressive accuracy even for low quantum numbers.

It is well known that virtual pairs of elementary particles appear briefly as vacuum fluctuations and then annihilate each other<sup>(2)</sup>. Many effects of these Virtual Antiparticle Pairs (VAPs) are well understood, such as the phenomenon of screening of “bare” electric charge by vacuum polarization of virtual fermions<sup>(3)</sup>. Can semiclassical models of VAPs be constructed? The test of usefulness of such a semiclassical model for a VAP should be whether the model successfully predicts the state’s lifetime in agreement with quantum theory.

The quantum states of normal material particles obey the Heisenberg Uncertainty Principle for energy ( $\Delta\varepsilon \Delta t \geq \hbar/2$ )<sup>(4)</sup> VAPs are ephemeral quantum states which can only exist so long as  $\Delta\varepsilon \Delta t \leq \hbar/2$ . In general, the maximum lifetime of such a VAP (of any massive elementary particle species) is the Heisenberg lifetime

$$t_H = \frac{\hbar/2}{2mc^2} , \quad (1)$$

where  $m$  is the mass of one of the particles (cgs units are used in this paper).

The goal of this paper is to point out that, if one adheres carefully to the semiclassical method, then it can be used to compute VAP lifetimes in good agreement with the Heisenberg lifetimes. This shows not only that semiclassical modeling corresponds unexpectedly well with QFT, but also offers the advantage that the coupling constants appear explicitly in the new resulting formulae, so that we may solve for their values (since we know  $t_H$  from QFT, too).

As a tool for further physical insight into VAPs, or a conceptual or teaching aid, it would seem natural to apply a semiclassical dynamical model to the VAP (analogous to the Bohr hydrogen atom), if it could be appropriately quantized. Semiclassical

quantization is a well understood method<sup>(5)</sup>. The Bohr semiclassical model successfully yields so many physical properties of hydrogen and has such undisputed pedagogical value that it is still widely used in quantum mechanics texts. In addition, the semiclassical Bohr-Sommerfeld quantization method continues to produce new physical insights into quantum-mechanical problems, such as Brau's recent success at modeling meson spectroscopy using a Bohr-Sommerfeld treatment of constituent quarks<sup>(1)</sup>. Comparison between the prediction of such a dynamical model for VAPs and the Heisenberg lifetime (Eq. 1) might be instructive in relation to the differences between semiclassical and fully quantum-mechanical physics of VAPs. This expectation is encouraged by Brau's derivation of useful formulae for the dependence of some physical quantities on quantum numbers, which emerge from the semiclassical method but have not been obtainable from full quantum calculations. Curiously, there seems to be no trace in the literature of such a dynamical model of VAPs.

In this paper it is shown that semiclassical relativistic two-body theory can enable us to compute good approximations of the Heisenberg VAP lifetimes  $t_H$  for the massive leptons, the quarks, and electroweak bosons. The agreement of the results with QFT is very good, and suggests that the models provide useful insights into VAPs.

## 2. VIRTUAL MASSIVE LEPTON ANTIPARTICLE PAIRS

### 2.1 Dynamics Corresponding with the Feynman Diagram

Let us first consider a virtual electron-positron pair (VEPP) unperturbed by any external forces, using classical electrodynamics. In second-order QED, processes described by the Feynman diagram in Fig. 1(a) occur<sup>(6)</sup>. An electron with four-momentum  $p$ , a photon with four-momentum  $k$ , and a positron of four-momentum  $-p - k$  spontaneously appear from the vacuum at one spacetime point  $x_1 = (t_1, \mathbf{x}_1)$  and propagate to another spacetime point  $x_2$ , where they annihilate; energy and momentum are conserved (because the particles are "off mass shell")

We shall take the Feynman diagram in Fig. 1(a) as the basis for a classical dynamical model, and then ensure that an appropriate quantization condition is met (the usual semiclassical approach).

Of course it is not possible to model Fig. 1(a) perfectly in the classical framework. In the diagram, the particles and the timelike virtual photon are free, with the electromagnetic interaction only acting at the vertices at the top and bottom of the diagram. This is the usual QED perturbation-theory approach. In contrast, classical physics assumes that the particles move in a potential continuously over time; QED perturbation theory treats the interaction without reference to time dependence<sup>(8)</sup>. So we cannot expect the classical dynamical model to correspond with every feature of the diagram. Rather, the objectives here are to answer the following questions: (1) can such a VEPP appear, consistent with the classical principles? (2) what happens to the particles thereafter to determine their dynamics? and (3) is the system subject to reasonable quantization conditions as in the semiclassical method? The general viewpoint of this approach is that QED has led the way in showing us the occurrence of processes like Fig. 1(a) in nature, now that we know about these processes, we can investigate what non-perturbative theory might tell us about them – in this case, semiclassical non-perturbative theory.

Concerning question (1), antiparticle creation and annihilation have been reconciled with classical relativistic dynamics for a long time. The role of antiparticles in classical relativistic dynamics is sometimes misunderstood, because of the historical interpretation of negative-energy states in relativistic quantum mechanics as antiparticles. However, the natural appearance of antiparticles as particles in a state of motion such that  $d\tau = -dt/\gamma$  (where  $\tau$  is proper time and  $\gamma$  is the Lorentz factor) was realized by Stückelberg<sup>(9)</sup>; Costella et al.<sup>(10)</sup> give a clear exposition of the *positive* rest mass energy of antiparticles in classical relativistic theory (see also Trump and Schieve<sup>(11)</sup>). So particle/antiparticle properties are well defined and consistent with the classical principles. In

addition, classical pair creation has been studied, for example by Carati<sup>(12)</sup> in solutions of the well-known Abraham-Lorentz-Dirac equation. It should be clear that antiparticle pair creation and annihilation are accepted as consistent with classical relativistic dynamics in the way that the following model is developed.

According to the Feynman diagram, the electron and positron are each created at the *origin* of the center-of-mass (CM) coordinate system. At the exact instant of the particles' creation, both are at  $r = 0$ . In the CM frame the leptons then travel apart along a radial line with some initial velocity  $v_0$  (Fig. 1b), with a separation  $R(t) = 2r$ . This motion is consistent with the usual theory, since the particles are off mass shell so that momentum is conserved. Because the electromagnetic potential is singular at  $R = 0$ , it appears at first as if the pair would be inseparable, due to infinite attraction and couldn't escape from the origin. Let us assume that each particle appears at some finite distance from the origin so that their initial separation is  $R_{int}$ , and for the moment let us ignore this obstacle. We shall have to let  $R_{int} \rightarrow 0$  to faithfully model the Feynman diagram, and we shall find later that  $R_{int}$  may be taken to zero in the computations.

Sometimes the appearance of a VAP is regarded as a violation of the conservation of energy on a timescale too brief to observe. That is true of the particles' rest mass energy, but since the particles are off mass shell and energy is conserved, the total energy of the particle-field system must be zero in QED (it was zero for  $t < t_1$ ). In this semiclassical model also, we must consider energy conserved (including rest mass), and assume that after the leptons' emission from the origin, the sum of their rest mass energy and kinetic energy is the negative of the electromagnetic binding energy at the separation  $R = 2r$  of the particles, requiring the two-body system energy equation

$$\varepsilon_v = 2\gamma m_e c^2 + U(R) = 0 \quad (2)$$

where  $\gamma = 1/\sqrt{1 - (v(r,t)/c)^2}$  is the Lorentz factor (as  $v \rightarrow c$ ,  $\gamma \rightarrow \infty$ ; as  $v \rightarrow 0$ ,  $\gamma \rightarrow 1$ ), and  $U(R)$  is the potential energy function of the electron and positron's mutual electromagnetic attraction. Thus our model has zero net energy in the CM frame

of reference<sup>(13)</sup>, and thus it costs the vacuum no net energy to create these particles. In fact, this is necessary for consistency with the semiclassical approach, which dictates conservation of energy in the dynamical model.

Another way to write eq. (2) makes the difference between VAPs and “real” pairs more explicit. As expressed by Greiner<sup>(4)</sup>: if a virtual pair is separated during the interval  $t_H$  and if it has gained more energy than  $2mc^2$ , then the particles become real. This is easily exhibited since the usual kinetic energy of an electron is  $T_e = (\gamma - 1)m_e c^2$ , so eq. (2) may be rewritten

$$T + U = 2(\gamma - 1)m_e c^2 + U = -2m_e c^2 .$$

The definition of energy baseline in Eq (2) captures in a classical way the energy debt that would have to be paid in order for these leptons to be escalated into free particles. The virtual quantum system evolves as if it were in a potential energy well of depth  $2m_e c^2$  lower than a “real” pair of particles would be.

In this model, we shall ignore radiation reaction, since in QED these particles are not capable of emitting radiation (and if the particles radiated, then we would be modeling some other, more complex process than Fig. 1(a)) We impose conservation of angular momentum, so that the spins of the particles are such that they sum to zero net angular momentum (the virtual photon is only a carrier of energy, but not of momentum or net angular momentum). Then the spin angular momentum of the electron must be antiparallel to that of the positron, and the magnetic moments  $\mu_{e-}$  and  $\mu_{e+}$  must be parallel

What forces determine the dynamics of these particles? With zero orbital angular momentum in the system, there are only the electrostatic and magnetic spin-spin forces in play (gravity can be ignored). In the rest frame of each lepton, the electrostatic potential is  $-e^2/R$  and the magnetic spin-spin potential is the magnetic field gradient potential energy  $U_B$  (see Ref 14), which gives the familiar field gradient force  $\nabla(\boldsymbol{\mu} \cdot \mathbf{B}) = \nabla(-U_B)$  (conventionally ignored in discussing the diagram in Fig. 1(a)).

What are the relative magnitudes of the two electromagnetic forces? To answer this, we need to estimate the maximum separation vector between the electron and positron. Conventionally, an upper bound is calculated for the separation of the electron and positron, which cannot move apart faster than  $c$ , the speed of light. Then an upper bound on their separation<sup>(15)</sup> is  $ct_{He}$ , with  $t_{He}$  given by (recall Eq. 1)

$$t_{He} = \frac{\hbar/2}{2m_e c^2} \approx 3.2 \times 10^{-22} \text{ s} .$$

Then  $ct_{He} = \hbar/(4m_e c) \approx 10^{-11} \text{ cm}$ .

Let us consider first the case in which the electron and positron separate along the direction of  $\mu_{e-}$ . The absence of torques ensures that the motion is purely one-dimensional. At maximum separation, the potential energy of the spin-spin interaction is  $U_B = -\mu \cdot \mathbf{B} = -2\mu_e^2/R^3$ , where

$$\mu_e = \frac{ge}{2m_e c} \frac{\hbar}{2} \approx 2e ct_{He} , \quad (3)$$

and  $g$  is the Landé factor  $\approx 2$  for fermions. Then the ratio of the potentials is

$$\frac{U_B}{V_e} = \frac{2\mu_e^2}{R^3} \frac{R}{e^2} = \approx 8 \left( \frac{ct_{He}}{R} \right)^2 .$$

For  $R = ct_{He}$ , the magnetic force is dominant. Although this differs from the usual QED model for VEPPs, it should be noted that this creates no conflict whatever between the present model and QED, because diagrams like Fig 1(a) do not contribute to any observable effect in QED<sup>(3)</sup>, other diagrams (processes) in which VAPs interact with other particles lead to the observable effects.

Perhaps it should be noted for comparison that a VEPP is a very different bound state of the electron and positron from positronium<sup>(16)</sup>; an electron and positron in a positronium state are in a stationary state with spatial extent of order  $a_0 \approx 0.53 \times 10^{-8} \text{ cm}$  (Bohr radius), whereas the leptons in a VEPP are not. The much smaller scale of the VEPP and the  $1/R^3$  dependence of the spin-spin force are the reasons that the



spin-spin force dominates in this VEPP model, although it is usually a small perturbation.

Let us assume that the leading term in the potential is the spin-spin force between the leptons, and solve for the dynamics using this term alone; we will then check to verify whether this assumption is accurate.

As the particles separate, the electromagnetic attraction between the leptons will slow their motions until they reach a maximum separation  $R_{max}$  where the velocity and kinetic energy are zero. While the particles move, we must perform a Lorentz transformation from the lepton rest frame to the CM frame, so  $U(R) = -2\mu_e^2/(\gamma R)^3$  (Jackson<sup>(17)</sup> explains how this introduces a change from  $R$  to  $\gamma R$  for this one-dimensional motion). When the particles come to rest at the turning points, it is easy to solve the energy equation (2) because  $\gamma = 1$ , and obtain

$$R_{max} = \left( \frac{\mu_e^2}{m_e c^2} \right)^{1/3} = \left( \frac{r_e \lambda_c^2}{16\pi^2} \right)^{1/3} = \left( \frac{e^2 \hbar^2}{4c} \right)^{1/3} \frac{1}{m_e c} \approx 4.70 \times 10^{-12} \text{ cm}, \quad (4)$$

where  $r_e = e^2/(m_e c^2) \approx 2.82 \times 10^{-13}$  cm is the “classical electron radius”, and  $\lambda_c = h/(m_e c) \approx 2.43 \times 10^{-10}$  cm is the Compton electron wavelength.

We see that  $R_{max} \approx ct_{He}/2$ , which is quite consistent with the conventional upper bound on the leptons’ separation derived from QED, and mentioned previously.

It should be noted that any structure in the pointlike electron or positron is known to be smaller than  $10^{-15}$  cm, as determined from high-energy scattering<sup>(18)</sup>, so the scale of our model is more than three orders of magnitude larger than any of the constituent particles’ structure, justifying our treating the leptons as points. (We now explicitly assume  $R_{int} \ll R_{max}$ .)

At the scale  $R_{max}$ , the strength of the electrostatic potential  $V_e(R) = -e^2/R$  is small relative to  $U_B(R)$ . Their ratio is  $U_B/V_e \approx 33$  at  $R = R_{max}$  (and greater for  $R < R_{max}$ ). The lepton motion in this model is governed by the spin-spin force, and the electrostatic potential is negligible in determining the dynamics.

After the leptons reach their turning points, we then expect that the electron and positron each retrace their motions in reverse and annihilate one another when they collide at the origin. The motions of the particles can be computed by integrating the energy equation (2), and we can compare the dynamical result (which we shall call  $t_{ve}$ ) with the quantum mechanical maximum timescale for this process of creation and annihilation in the presence of no external forces (the Heisenberg lifetime),  $t_{He}$ . There is a considerable literature of attempts to solve rigorously the classical problem of colliding relativistic charged particles<sup>(19)</sup>; no results are found in the literature for the problem considered here.

Let us also address one conceivable objection to the physical applicability of this model. It is well known that a free electron cannot be localized in a wave packet smaller than  $\Delta x_Z \sim \lambda_c/2\pi$ , due to the *Zitterbewegung*<sup>(20)</sup> (oscillations in  $\langle x \rangle$  with frequency  $\omega_Z = 2mc^2/\hbar \approx 1.5 \times 10^{21} \text{sec}^{-1}$ ) Although  $R_{max} \ll \Delta x_Z$ , the period of *Zitterbewegung* oscillations is  $4.2 \times 10^{-21} \text{ s} \gg t_{He}$ , so in QED the *Zitterbewegung* does not have time to delocalize the VEPPs before they annihilate; we shall see below whether the same is true in our dynamical model.

## 2.2 Solving the Equation of Motion

Let us calculate the dynamical timescale for the VEPP creation-annihilation process, using the energy equation (2) as an equation of motion. We can rewrite the energy equation as

$$\gamma^4 = \left( \frac{R_{max}}{2r} \right)^3.$$

To write the above in dimensionless form, let us define  $\zeta = R/R_{max}$ . Taking the square root of both sides of the energy equation, we obtain

$$\gamma^2 = \left( \frac{R_{max}}{R} \right)^{\frac{3}{2}} = \zeta^{-\frac{3}{2}}$$

Invert both sides and expand  $\gamma$ :

$$1 - \frac{v^2}{c^2} = \zeta^{\frac{3}{2}}$$

Solve for  $v$ :

$$v = c\sqrt{1 - \zeta^{\frac{3}{2}}} = \pm \frac{dr}{dt}$$

$$dt = \pm \frac{dr}{c\sqrt{1 - \zeta^{\frac{3}{2}}}},$$

an equation of motion which may be integrated.

Let the total time for the formation, separation and re-annihilation of the virtual  $e^+e^-$  pair be denoted  $t_{ve}$ , the dynamical lifetime. Then  $t_{ve}$  is twice the time for the particles to separate and reach the turning points, since the path is approximately time-symmetric. For the purpose of this calculation, we can let  $R_{int} \rightarrow 0$  without encountering a singularity, and the model now corresponds to the Feynman diagram without depending upon a free parameter  $R_{int}$ . Then

$$t_{ve} = 2 \frac{1}{c} \int_0^{R_{max}/2} \frac{dr}{\sqrt{1 - \left(\frac{2r}{R_{max}}\right)^{\frac{3}{2}}}} = \frac{R_{max}}{c} \int_0^1 \frac{d\zeta}{\sqrt{1 - \zeta^{\frac{3}{2}}}}.$$

The integral may be found in ref. 21; substituting its value yields the dynamical VEPP lifetime

$$t_{ve} = \frac{R_{max}}{c} \left( \frac{\sqrt{\pi} \Gamma(\frac{2}{3})}{6 \Gamma(\frac{7}{6})} \right) \approx \frac{R_{max}}{c} (1.7247) = \left( \frac{e^2 \hbar^2}{4c} \right)^{1/3} \frac{1.7247}{m_e c^2} \approx 2.70 \times 10^{-22} \text{ s}. \quad (5)$$

Let us compare this dynamical lifetime with the Heisenberg lifetime for such an electron-positron pair,  $t_{He} = \hbar/(4m_e c^2) \approx 3.2 \times 10^{-22}$  s above. The dynamical computation is 16% lower. Since  $t_{ve} \approx t_{He}$ , there is clearly no difficulty for the model posed by *Zitterbewegung*, in agreement with QED.

We were trying to obtain the *maximum* lifetime of such a dynamical system, and the reader may wonder whether  $t_{ve}$  is in fact a maximum. If the electron and positron separated along some trajectory different from the torque-free axis of their angular momenta (which we used in the above calculation), what would the lifetime be? Let us

refer to Fig. 2. Let us suppose that the electron and positron initially separate along a line with a direction at an angle  $\theta$  relative to the  $\mu$  vector. If  $\theta = 90^\circ$ , then  $U_B = -\mu \cdot \mathbf{B} > 0$  and the energy equation (2) does not have solutions because the potential is repulsive, not attractive. The semiclassical model suggests that VEPPs do not exist with motions along these trajectories. The cones such that  $\theta \approx 54.7^\circ$  define the surface outside which  $U_B > 0$ , as shown in Fig. 2. Inside the cones, as  $\theta$  decreases  $\mu \cdot \mathbf{B}$  becomes positive ( $U_B$  becomes negative) and it becomes possible to satisfy Eq. (2) iff  $\mu \cdot \mathbf{B} > 2m_e c^2$ .

The dynamics of the VEPP are more complex for  $0 < \theta < 54.7^\circ$  than in the  $\theta = 0$  case, which we already treated. Let us consider an electron near the vertical axis, as pictured in Fig. 2, such that  $0 < \theta \ll 54.7^\circ$ . There is now a torque on the magnetic dipole moment of the electron, given by  $\tau = \mu \times \mathbf{B}$ . Classically this causes the magnetic moment to precess about  $\mathbf{B}$ . But by symmetry (and conservation of angular momentum) the positron experiences the same torque due to the electron's magnetic field, and hence both magnetic moments precess equally and remain always parallel. Because  $\mu$  and  $\mathbf{B}$  are no longer parallel,  $|\mu \cdot \mathbf{B}|$  is reduced. If the trajectories of the electron and positron are still close to the vertical axis,  $R$  in the particle frame still is approximately  $\gamma R$  in the CM frame, and we can use  $U_B = -\mu_e^2(3\cos^2\theta - 1)/(\gamma R)^3$  in Eq (2)<sup>(22)</sup>. As  $\theta$  increases from 0 to larger values, this leads to smaller values of  $R_{max}$  and  $t_{ve}$ , and thus we see that the values for these parameters computed first above are indeed maximal as desired.

We see that the conservation laws uniquely determine the dynamical model that yields  $t_{ve}$  classically, giving us a new derivation of  $t_{He}$  to good approximation. It will be demonstrated below that the agreement of  $t_{ve}$  and  $t_{He}$  is no coincidence, but results from valid physical relationships.

Let the numerical factor involving the ratio of  $\Gamma$  functions in eq. (5) be designated  $f_s \approx 1.72$ . Note that for the ratio

$$\frac{t_{He}}{t_{ve}} = \frac{\hbar}{4} \frac{1}{f_s} \left( \frac{4c}{e^2 \hbar^2} \right)^{1/3} \approx 1.16$$

$m_e$  cancels out, so this form of VAP lifetime derivation works for all of the massive lepton VAPs (electron-positron, muon-anti-muon and tau-anti-tau leptons), irrespective of their masses (as it must to be valid). The muon and tau lepton, of course, have smaller values of  $R_{max}$  and  $t_v$  because of their larger masses, and  $t_{v\mu} \approx t_{H\mu}$ ,  $t_{v\tau} \approx t_{H\tau}$  to the same relative precision. (See Table I.)

These results show that this semiclassical model gives remarkable agreement with the QFT lifetimes of VEPPs, in view of the model's simplicity (only point magnetic dipole particles interacting via a potential function in one dimension). But the reader may wonder whether this is coincidental. And what about the quantization that is necessary to make it really "semiclassical" rather than entirely classical? Next the quantization will be addressed, and an independent physical derivation of the VEPP quantization will be presented.

### 2.3 Quantization Condition is Met

The Bohr model was quantized using conditions on the angular momentum of the orbiting electrons in a non-relativistic case<sup>(23)</sup>. In the present model, however, the orbits have vanishing angular momentum and angular momentum conservation has already been imposed to determine the orientations of the  $\mu_{e-}$  and  $\mu_{e+}$ . Hence the Bohr approach is not exactly applicable in this VEPP model.

Let us consider the quantization of the electromagnetic field in the VEPP. The well-known zero-point field energy of the electromagnetic field is  $\varepsilon_{em} = \frac{1}{2}\hbar\omega$ . That is, for any wave mode of angular frequency  $\omega$ , there is a vacuum fluctuation energy  $\varepsilon_{em}$ . Another way to view this fact is that there is a quantization of any zero-point fluctuation mode  $\omega$  such that its energy is proportional to the *action*  $\frac{1}{2}\hbar$ . (Quantization of action is a fundamental connection from classical mechanics to quantum mechanics, and was actually used to derive the Schrodinger equation from the principle of least action by Feynman<sup>(24)</sup>.) Since the VEPP induces an electromagnetic vacuum fluctuation, let us calculate the action associated with the electromagnetic field in the VEPP over its cycle

from creation to annihilation

The expression for the action associated with a potential  $U$  acting on a particle is given (for the relativistic case) by Lanczos<sup>(25)</sup>

$$\mathcal{A} = - \int_{t_1}^{t_2} U \frac{ds}{c} ,$$

where  $ds = c dt/\gamma$ . It follows that the action integral of the VEPP electromagnetic field is (recall the time symmetry relative to the turning point at  $t_{ve}/2$ ):

$$\begin{aligned} \mathcal{A} &= -2 \int_0^{t_{ve}/2} \left( -\frac{2\mu_e^2}{c\gamma^3 R^3} \right) \frac{c dt}{\gamma} = 4\mu_e^2 \int_0^{t_{ve}/2} \frac{dt}{\gamma^4 R^3} = 4\mu_e^2 \int_0^{R_{max}/2} \frac{dr}{c \gamma^4 R^3 \sqrt{1 - \zeta^{3/2}}} \\ &= \frac{4\mu_e^2}{c R_{max}^3} \frac{R_{max}}{2} \int_0^1 \frac{d\zeta}{\gamma^4 \zeta^3 \sqrt{1 - \zeta^{3/2}}} = \frac{2\mu_e^2}{c R_{max}^2} \int_0^1 \frac{d\zeta}{\zeta^{-3} \zeta^3 \sqrt{1 - \zeta^{3/2}}} \\ &= \frac{2m_e c}{R_{max}^2} \frac{\mu_e^2}{m_e c^2} \int_0^1 \frac{d\zeta}{\sqrt{1 - \zeta^{3/2}}} = 2m_e c^2 \frac{R_{max}}{c} f_s = 2m_e c^2 t_{ve} = 2 \left( \frac{e^2 \hbar^2}{4 c} \right)^{1/3} f_s. \quad (6) \end{aligned}$$

This final result<sup>2</sup> is approximately  $4.4 \times 10^{-28}$  erg s, 16% less than  $\frac{1}{2}\hbar$ . Thus the model is *inherently quantized* (to within the 16% difference in  $t_{ve}$ ), and is the corresponding semiclassical model for VEPPs.

In the following sections it will be seen that when the same semiclassical method of modeling is applied to quark-antiquark virtual pairs, the same agreement in the quantum mechanical and semiclassical timescales results, as well as the action integral.

---

<sup>2</sup> This action integral for our model VEPP potential equals the conventional zero-point field action, to good approximation. N.B: if  $t_{ve}$  exactly equalled  $t_{He}$ , then  $\mathcal{A}$  would exactly equal  $\frac{1}{2}\hbar$ . In Section 6. below an interpretation of this is given.

### 3. VIRTUAL QUARK ANTIPARTICLE PAIRS

#### 3.1 Dynamics Corresponding with the Feynman Diagram

The method of Sec. 2 can be applied to quark-antiquark virtual pairs. A process analogous to Fig. 1(a) exists in Quantum Chromodynamics (QCD), but with a gluon replacing the timelike photon<sup>(26)</sup>. The energy equation is of the same form,

$$\varepsilon_q = 2\gamma m_q c^2 + U(R) = 0, \quad (2')$$

except that the dominant force is the “color” force instead of the spin-spin electromagnetic attraction. The potential function  $U(R)$  has been inferred from decades of high-energy scattering experiments. Mesons like the  $J/\psi$  particle are bound states of a quark and its anti-quark, and high-energy particle collision experiments have established phenomenological forms of  $U(R)$ . These experiments have revealed that a useful empirical form of the potential is the so-called “Cornell funnel potential”<sup>(27)</sup>

$$V(R) = -\frac{\kappa}{R} + aR,$$

where  $\kappa \approx \frac{4}{3}\alpha_s$ , and the QCD strong coupling strength  $\alpha_s \sim 0.2$  in “natural units” (units such that  $\hbar = c = 1$ ), and  $a \approx 0.25 \text{ GeV}^2$ . Converted to cgs units used herein,  $\kappa \sim 8.6 \times 10^{-18} \text{ erg cm}$ . The second term,  $aR$ , is only significant for  $R > 10^{-13} \text{ cm}$ , so we will not need to consider it, since the first term with the Coulomb-like dependence will strongly dominate the potential for the range of  $R_{max}$  of quark VAPs. The Coulomb-like term is due to exchange of a vector gluon between the quark and antiquark<sup>(27,28)</sup>. (There are other empirical forms of the quark-antiquark potential – many discussed in Ref. 27 – but the Cornell potential will be sufficient for present use. Also, it should be mentioned that the light up and down quarks are not as accurately treated with this kind of potential model as the heavier quarks; nevertheless, it is well known that potential models work surprisingly well in describing the dynamics of all but the lightest quark flavors.)

The QCD coupling coefficient  $\alpha_s$  is not constant, but is a “running coupling” because of its variation with 4-momentum transfer  $q$  of the interacting particles<sup>(29)</sup>. This can be allowed for in our semiclassical model. However, it is important to be clear about what this two-body model can be expected reasonably to correspond with in QCD. The QCD coupling strength  $\alpha_s(q)$  has been calculated to four-loop order<sup>(30)</sup>, including a series of processes (diagrams) with numerous topologies. But the present semiclassical model only consists of the spacetime structure of a single-loop process. Hence it is not applicable to processes in which more than one loop are involved. It makes sense to compare the two-body model here only with lowest-order QCD (and corrections with the same spacetime diagram, such as spin-spin or electrostatic corrections). By the same token, in QFT a quark VAP doesn’t include those multiple-loop processes, so QFT logic prohibits using multiple-loop processes to compute  $t_{Hq}$  for quarks also.

First, to demonstrate the basic physical model, let us take  $\alpha_s = 0.20$ , sometimes called the “canonical” value<sup>(27)</sup>, derived from a fit of the charmonium system. Let us calculate the dynamical timescale for a charm quark-antiquark VAP using this single value of  $\alpha_s$ . After that, we will then generalize the model to account for the running of  $\alpha_s$  as a function of  $q$ .

Here is the semiclassical dynamical timescale calculation: including a Lorentz factor  $\gamma$  appropriate for the  $1/R$  color-Coulomb function (to make the Lorentz transformation to the CM frame<sup>(17)</sup>), the potential in Eq (2') becomes

$$U(R) = -\frac{\kappa}{\gamma R} .$$

As in Sec. 2, we can solve (2') for  $R_{max}$  at the turning point

$$\begin{aligned} 2 m_q c^2 &= -U(R_{max}) = \frac{\kappa}{R_{max}} \\ R_{max} &= \frac{\kappa}{2 m_q c^2} . \end{aligned} \tag{4'}$$

For the charm quark constituent mass of  $1.5 \text{ GeV}/c^2 = 2.7 \times 10^{-24} \text{ g}$ , we find the charm quark VAP has an  $R_{max} = 1.7 \times 10^{-15} \text{ cm}$ . This means that the quarks are deep in



the color-Coulomb part of the potential, and the  $aR$  term of the Cornell potential is insignificant in magnitude (as is the electrostatic potential). The dynamics are determined by the single vector gluon exchange, not the multi-gluon exchange of confinement in the linear region, in agreement with QCD<sup>(28)</sup>.

For the dynamical timescale, we rewrite the energy equation (2') as  $\gamma^2 = \zeta^{-1}$ , with  $\zeta = R/R_{max}$ , and find

$$\begin{aligned} t_{vq} &= 2 \int_0^{R_{max}/2} \frac{dr}{c\sqrt{1-\zeta}} = \frac{R_{max}}{c} \int_0^1 \frac{d\zeta}{\sqrt{1-\zeta}} \\ &= \frac{R_{max}}{c} \frac{\sqrt{\pi} \Gamma(1)}{\Gamma(\frac{3}{2})} = \frac{R_{max}}{c} f_c = \frac{f_c \kappa}{2m_q c^3} \end{aligned} \quad (5')$$

where we label the  $\zeta$  integral's value as  $f_c \approx 2.0$ . For the charm quark, with  $m_q \approx 2.7 \times 10^{-24}$  g, we  $t_{vq} \approx 1.3 \times 10^{-25}$  s.

For comparison, the Heisenberg lifetime of the charm quark is  $t_{Hq} \approx 1.1 \times 10^{-25}$  s, about 14% lower.

Considering the quantization of the color force potential field in a virtual charm quark-antiquark pair, we compute the field action over the VAP lifetime:

$$\begin{aligned} \mathcal{A} &= -2 \int_0^{t_{vq}/2} \left( -\frac{\kappa}{c\gamma R} \right) \frac{c dt}{\gamma} = \frac{2\kappa}{c} \int_0^{R_{max}/2} \frac{dr}{\gamma^2 R \sqrt{1-\zeta}} \\ &= \frac{\kappa}{c} \int_0^1 \frac{d\zeta}{\zeta^{-1} \zeta \sqrt{1-\zeta}} = \frac{\kappa}{c} \int_0^1 \frac{d\zeta}{\sqrt{1-\zeta}} \\ &= \frac{\kappa}{c} f_c \approx \frac{2\kappa}{c} \approx 5.6 \times 10^{-28} \text{ erg s} \approx 0.53 \times \hbar \end{aligned} \quad (6')$$

This action integral is a good approximation to the zero-point fluctuation action,  $\frac{1}{2}\hbar$ , and means that this version of the model, too, is inherently quantized just as the electromagnetic case was in Sec. 2. N.B: if  $t_{vq}$  exactly equalled  $t_{Hq}$ , then  $\mathcal{A}$  would exactly equal  $\frac{1}{2}\hbar$ .

### 3.2 Generalization to Running Coupling $\alpha_s(q)$

The above results illustrate the basic application of the model to a quark VAP for which  $\alpha_s$  was determined from experiments with real (non-virtual) bound states of that quark. But to make the model realistic for quarks in general, the running coupling  $\alpha_s(q)$  must be included in the model, not just one universal value of  $\alpha_s$ . We can develop the model to account for the running coupling if we can include a characteristic  $q$  for the VAP of each quark flavor

The QCD running coupling is a function of momentum transfer  $Q^2 = -q^2$ . A standard way to incorporate asymptotic freedom is to let  $\alpha_s$  depend on the quark masses and use  $-q^2 = (m_1 + m_2)^2$ , with the  $m_i$  the quark masses<sup>(28)</sup>. Then we may use Richardson's expression<sup>(31)</sup>

$$\alpha_s(q) \sim \frac{12\pi}{33 - 2n_f} \frac{1}{\ln(-q^2/\Lambda^2)} , \quad (7)$$

where  $n_f$  is the number of quark flavors with masses much less than  $m_1 + m_2$ , and  $\Lambda$  is the QCD scale energy, approximately 0.22 GeV.

The parameter  $n_f$  varies as described above because we are using an effective field theory obtained by integrating out all quarks heavier than the typical energy under consideration<sup>(32)</sup>. I.e.,  $n_f$  is the integer such that there are  $n_f$  quarks with masses much less than  $2m_q$ ; for this paper  $n_f$  will be defined as the number of quarks with masses of  $2m_q/10$  or less. We now can use  $m_1 = m_2 = m_q$  in the expression for  $-q^2$  and compute  $\kappa$  from eq. (7) more realistically for a running coupling. The results for this running color-Coulomb force model, with  $\alpha_s(q)$  given by Eq. (7), appear in Table I (marked with the symbol © to indicate "Color Only").

We see that the semiclassical lifetimes  $t_{vq}$  of the quark VAPs all agree with the Heisenberg lifetimes  $t_{Hq}$  from QFT to within a factor of about 2.8, and much better for the charm and bottom quarks. While this agreement isn't as good as for the lepton VAPs in Sec. 2, the semiclassical model is still in rough agreement with QCD, to much better than an order of magnitude. The color-Coulomb potential from QCD, when

taken as a classical force strength, leads to dynamical timescales of VAPs that correspond surprisingly well with the QFT lifetimes for the VAPs. In addition, the values of  $R_{max}$  are consistent with VAP size scales that are deep within the color-Coulomb part of the potential function (not out in the linear region where the theory would be inappropriate). This needn't be a total surprise in view of Brau's<sup>(1)</sup> recent success modeling mesons semiclassically, but the present work is the first semiclassical treatment of quark VAPs.

### 3.3 Combined Color-Coulomb and Spin-spin Interaction Models

The modeling of quark VAP lifetimes can be taken as a qualified success, but it is possible to go further with this model and include the effects of spin-spin interactions between the quark-antiquark pairs. As noted by Lichtenberg<sup>(33)</sup>, the spin-spin interaction between quarks is the source of electromagnetic mass splittings among hadron isospin multiplets. In the present semiclassical model, because the quark VAPs have sufficiently small  $R_{max}$  values, the spin-spin energy can be comparable with the color-Coulomb potential for the heavier quarks in which asymptotic freedom reduces  $\alpha_s(q)$ . Let us include the spin-spin potential in the quark VAP energy Eq. (2') and examine the effect on  $t_{vq}$ .

$$U(R) = -\frac{\kappa}{\gamma R} - \frac{2\mu_q^2}{(\gamma R)^3} ,$$

where

$$\mu_q = \frac{gQ_q}{2m_q c} \frac{\hbar}{2}$$

is the magnetic moment of a quark with charge  $Q_q$ . The energy equation becomes

$$\varepsilon_q = 2\gamma m_q c^2 - \frac{\kappa}{\gamma R} - \frac{2\mu_q^2}{(\gamma R)^3} = 0 . \quad (2'')$$

Again we can derive the turning point separation  $R_{max}$  by letting  $\gamma \rightarrow 1$ . This is easily done by defining  $\zeta$  in terms of the scale length from the previous case which considered only the color-Coulomb force.

$$\zeta = \frac{R}{\kappa/(2m_q c^2)} .$$

With this substitution, the energy equation with  $\gamma = 1$  becomes

$$\zeta_{max}^3 - \zeta_{max}^2 - \Delta = 0 \quad \text{with} \quad \Delta \stackrel{\text{def}}{=} \frac{2(Q_q \hbar c)^2}{\kappa^3} . \quad (4'')$$

The parameter  $\Delta$  is a measure of the importance of the spin-spin potential relative to the color-Coulomb potential;  $\Delta \rightarrow 0$  recovers the previous case of color-Coulomb potential dynamics only. There is only one real root of the cubic equation, and it is solved for  $\zeta_{max}(\Delta) \geq 1$  where  $\Delta$  is found from  $\kappa = \frac{4}{3}\alpha_s$ . The values of  $\alpha_s$  are tabulated in Table I

To obtain the VAP dynamical lifetime in the case that both color-Coulomb and spin-spin potentials are significant, the general energy equation is

$$\gamma^4 \zeta^3 - \gamma^2 \zeta^2 - \Delta = 0 ,$$

which is a simple quadratic in  $\gamma^2$  with solutions

$$\gamma^2 = \frac{1}{2\zeta} \left( 1 \pm \sqrt{1 + \frac{4\Delta}{\zeta}} \right) = \frac{1}{1 - \beta^2} .$$

Only the positive root is physically significant. This leads to

$$1 - \beta^2 = 2\zeta \left( 1 \pm \sqrt{1 + \frac{4\Delta}{\zeta}} \right)^{-1}$$

$$\beta = \sqrt{1 - \frac{2\zeta}{1 + \sqrt{1 + \frac{4\Delta}{\zeta}}}} = \frac{v}{c} = \frac{1}{c} \frac{dr}{dt}$$

$$dt = \frac{dr}{c} \frac{1}{\sqrt{1 - \frac{2\zeta}{1 + \sqrt{1 + \frac{4\Delta}{\zeta}}}}} .$$

The only difference in the limits of integration from the color-Coulomb-only case is that the upper limit becomes  $\zeta_{max} \geq 1$  instead of just 1. The dynamical timescale then becomes

$$t_{vq} = \frac{\kappa}{2m_q c^3} \int_0^{\zeta_{max}} \frac{d\zeta}{\sqrt{1 - \frac{2\zeta}{1 + \sqrt{1 + \frac{4\Delta}{\zeta}}}}} .$$

This expression reduces to the previous one (Eq. (5')) when  $\Delta = 0$ .

For each of the six quarks, one computes  $\Delta(\alpha_s)$ , the value of the dimensionless turning point separation of the quarks  $\zeta_{max}$  from the root of Eq. (4''), and then  $t_{vq}$  is given by the above expression with  $\zeta_{max}$  as the upper limit of integration. The integral is simple to perform numerically (a short C program for this is available from the author upon request). The results are tabulated in Table I, next to the  $t_{Hq}$  values.

It can be seen that the spin-spin interaction has insignificant effect on  $t_{vq}$  for the light down, up and strange quarks. Because of asymptotic freedom the QCD coupling weakens for the heavier quarks, however, and the spin-spin correction comes into play, increasing  $R_{max}$  over what it would be in the case of the color-Coulomb potential alone. The top quark VAP, with  $\Delta \approx 2.0$ , is dominated by the spin-spin potential rather than color-Coulomb. The net effect of including both potentials is to improve the agreement of  $t_{vq}$  with  $t_{Hq}$  significantly for the top quark, but increase the discrepancy slightly between the model and Heisenberg lifetimes for the charm and bottom VAPs. The model lifetimes  $t_{vq}$  for charm, bottom, and top quark VAPs differ from the Heisenberg values by 37%, 7%, and 9%, respectively. Including spin-spin attraction has insignificant effect on the model lifetimes for the down, up, and strange quarks, which differ by factors of 2.8, 2.8, and 2.0 respectively from the Heisenberg values. Potential models for these light quarks are well-known to be generally poorer than for the heavy quarks<sup>(27)</sup>.

#### 4. VIRTUAL WEAK BOSONS

The third class of elementary particles to which we can apply this model are the weak interaction gauge bosons  $W^\pm$  and  $Z^0$ . These particles are believed to be non-composite and point-like. It would be interesting if we could use the virtual weak boson-antiboson pairs to probe the weak interaction, but our model requires that we use as the potential the strongest force to which the particles respond; in this case, the weak bosons interact by the electromagnetic spin-spin force as well as the weak force (which

is of order  $10^{30}$  times weaker than the electrostatic attraction of the antiparticles in low-energy interactions<sup>(34)</sup>) Consequently the potential that we must use is the spin-spin interaction between two massive bosons via their spin magnetic moments:

$$\mu_W = \frac{ge}{2m_W c} \hbar, \quad (3')$$

where the factor  $g \approx 1$  can be assumed for bosons.

The form of Eq. (3') for the magnetic moment is therefore the same as Eq (3), except for the substitution of the  $W$  or  $Z$  mass for a lepton's mass, and so the subsequent mathematics is the same as in Sec. 2. (We may wonder whether the  $Z^0$  has a magnetic moment like the electrically neutral neutron, but if so, then the present model would seem to be applicable.) We find that the dynamical timescale  $t_{vW}$  is again 16% less than  $t_{HW}$ . The computation of the action is also 16% less than  $\frac{1}{2}\hbar$ . Therefore, this third type of elementary point-like massive particles also can be described approximately by this semiclassical model. (Results are in Table I.)

## 5. COMPOSITE PARTICLES AND THE BREAKDOWN OF THE MODEL

The models above were built around the dynamics of only two point-like bodies interacting through a simple potential. Consequently the models should not be expected to represent well the dynamics of composite particles like mesons and other hadrons. For instance, virtual pairs of anti-mesons comprise four quarks *in toto*, and this is no longer a two-body problem. Nucleons exhibit highly complex internal dynamics due to their comprising numerous valence quarks and virtual strange quarks<sup>(35)</sup>, so our models aren't applicable. If the two-body models that have been constructed above do not describe such multi-body VAPs, then that is no objection to the two-body models.

## 6. THE COUPLING CONSTANTS

Having found that the dynamical timescales in these models approximate well the Heisenberg lifetimes in these eleven cases – indeed, in all of the applicable cases of

known massive non-composite VAPs in nature – let us proceed with some reasonable derivations based on the observations  $t_H \approx t_v$  for each case.

### 6.1 The Unit of Charge $e$

The value of the action integral  $\mathcal{A}$  in the VEPP case (Sec. 2) implies that there is not just a fortuitous coincidence between the  $t_{He}$  and  $t_{ve}$  timescales. Rather, the VEPP model matches the expected action integral for a vacuum fluctuation, and this is no doubt because it reflects the physical process in a valid way. This agrees with standard QED, in which vacuum fluctuations of the positron-electron field generated by the electromagnetic field are the virtual creation and annihilation of VEPPs, and the fluctuations of the electromagnetic field generated by the VEPPs are the virtual emission and absorption of photons, as Schwinger explained<sup>(36)</sup>.

Since we know the equation for  $t_{He}$  from QFT, we may equate it with the semiclassical result in Eq. (5) to derive approximations for two familiar fundamental physical constants, the electric charge quantum  $e$  and the fine structure constant  $\alpha = e^2/(\hbar c)$ , in terms of  $\hbar$  and  $c$  only – a very interesting result. If we approximately equate  $t_{He} \approx t_{ve}$ , label the charge of a virtual positron  $e_v$  to denote the derived value, and solve for it, then we find easily that

$$e_v \approx \left( \frac{\hbar c}{16 f_s^3} \right)^{1/2} \approx 6.2 \times 10^{-10} \text{ esu.}$$

This is 30% high, compared with the usual measured value,  $e \approx 4.8 \times 10^{-10}$  esu. It is closer to the “bare” charge – what  $e$  would be if it were not “dressed” by the screening of vacuum fluctuations<sup>(37,38)</sup>. In fact, we should have expected that this calculation was likely to yield a result larger than the usual observable charge  $e$  because  $R_{max} \ll \lambda_c$ , the characteristic scale of the screening cloud of VEPPs which surrounds any free electron or positron. Different calculating methods lead to different estimates for the magnitude of the bare charge: ref. 37 gives a calculation suggesting that  $e_{bare}^2 \approx 1.08 e^2$ , but ref. 38

presents an argument based on the photon propagator, showing that the QED perturbation theory fails and  $e_{bare}$  could be infinite. If the semiclassical model in the present paper had led to a value for  $e_v$  less than the observable  $4.8 \times 10^{-10}$  esu, then the model would appear unphysical; however it is unclear whether the semiclassical approximation should be expected to hold to such precision. The value for  $e_v$  derived from this model is consistent with  $e_{bare}$  from QED, given present theoretical uncertainties.

We can also easily derive  $\alpha_v \approx 1/(16f_s^3) \approx 1/83$ ; this is 66% larger than the well-known  $1/137\,037$  value for  $\alpha$  (just because of the propagation of the 30% difference between  $e_v$  and  $e$ ). As pointed out in the preceding paragraph, our model tends to reflect the bare value of  $\alpha$ , not the usual observed value based on  $e$  for distances from a free electron that are large relative to  $\lambda_c$ .

## 6.2 The QCD Coupling $\alpha_s(q)$

The semiclassical model is successful at predicting  $t_{Hq}$  within 10% or better for the bottom and top quarks, so it is obviously possible to reverse the derivation, start from  $t_{vq} \approx t_{Hq}$  and derive  $\alpha_s(q)$  in the one-loop approximation of Eq. (7) for  $|q| = 2m_q c$  in the cases of the charm, bottom, and top quarks (that is,  $|q| = 3.0, 9.4$  and  $348$  GeV/ $c$ ). It is straightforward to pick a trial value of  $\alpha_s$ , calculate  $\Delta$  and  $\zeta_{max}$ , perform the numerical integral to compute  $t_{vq}$  accounting for both color and spin-spin potential terms, and iterate to a convergence of the predicted  $t_{vq}$  with  $t_{Hq}$ .

The prediction for the top quark of  $\alpha_s(348 \text{ GeV}/c) \approx 0.14$  is an interesting one from semiclassical theory, in an energy domain not yet reached by particle accelerators; it's about 27% greater than the 0.11 that Richardson's expression (eq. 7) predicts. For the bottom quark, the model implies  $\alpha_s(9.4 \text{ GeV}/c) \approx 0.18$ , about 5% less than eq. (7). For the charm quark, the derived value of  $\alpha_s(3 \text{ GeV}/c) \approx 0.15$  is approximately 32% less than the Richardson expression result, 0.22.

Although values of  $\alpha_s$  that are derived at the light quark masses are less accurate, they are still much better than order of magnitude. Since  $\Delta$  is small for the up,



down and strange quarks, the color-only formulae apply. To derive a value of  $\alpha_s$  from the model, eq. (5') with  $f_c = 2.0$  is set equal to  $t_{Hq}$ . This gives  $\alpha_s \approx 2.4 \times 10^{16} m_q c^3 t_{Hq} \approx 0.19$ . For the strange quark, this is 50% less than Richardson's value (eq. 7). For the up and down quarks, the model implies  $\alpha_s \approx 37\%$  of the Richardson value.

### 6.3 The Electroweak Bosons' Coupling

A separate weak interaction force constant cannot be derived from the model, even though we know  $t_{vW} \approx t_{HW}$ . In these cases, though,  $R_{max} \ll 10^{-14}$  cm, the electroweak unification scale<sup>(39)</sup>. The electroweak unification in the Standard Model at this scale means that it is reasonable for the dynamical model to behave the same as in the electromagnetic dynamical model of VEPPs and other massive lepton VAPs. The result here is then consistent with the Standard Model, given electroweak unification.

## 7. DISCUSSION

Let us summarize the results.

- (1) The dynamical timescale  $t_v$  predicted from VAP motions due to the electromagnetic spin-spin force approximately equals the Heisenberg lifetime of the VAP,  $t_H$ , within 16%, for the massive leptons.
- (2) The action integral of the electromagnetic spin-spin potential over the dynamical timescale approximately equals the zero-point field action,  $\hbar/2$ , within 16%, for the massive leptons
- (3) The dynamical timescale  $t_v$  predicted from VAP motions due to the quark-antiquark color-Coulomb and spin-spin forces approximately equals the Heisenberg lifetime of the VAP  $t_H$ , within 10% or better for the heaviest quarks (bottom and top), and within a factor of about 2.8 or better for the lighter quarks (down, up, strange and charm).
- (4) The action integral of the quark-antiquark color potential over the dynamical timescale approximately equals the zero-point field action  $\hbar/2$ , within 6%, for

the charm quark

- (5) The dynamical timescale  $t_v$  predicted from VAP motions due to the electromagnetic spin-spin force approximately equals the Heisenberg lifetime of the VAP  $t_H$ , within 16%, for the weak bosons.
- (6) The action integral of the electromagnetic spin-spin potential over the dynamical timescale approximately equals the zero-point field action  $\hbar/2$ , within 16%, for the weak bosons.

Several points should be noted about the above results:

- There are no free, adjustable parameters in any of the models.
- (2) does not follow trivially from (1) – i.e., the close agreement between  $\mathcal{A}$  and  $\hbar/2$  has a different mathematical origin than the agreement of  $t_v$  with  $t_H$ .
- (4) does not follow trivially from (3), similarly.
- (3) and (4) are independent of (1) and (2) because the color force potential is completely different in form from the spin-spin potential.
- (5) and (6) do not follow trivially from (1) and (2), because bosons and fermions have different spins which only lead to similar expressions for their magnetic moments incidentally.

There appears to be no way that these  $t_H$  and  $t_v$  values could all be so nearly equal by coincidence alone, much less for the field quantization conditions to magically come out satisfied by chance. In the case of the VEPP model, some algebraic dependence on  $\hbar$  exists in the formulae, but not in such a way as to account for the satisfaction of the quantization condition. The agreement between  $\mathcal{A}$  and  $\hbar/2$  suggests an important relationship between classical and quantum aspects of action. In the case of the quark-antiquark model, however, the color potential function is a purely empirical formula, with no algebraic relationship to  $\hbar$ , consequently, the agreement of  $\mathcal{A}$  and  $\hbar/2$  for the charm quark VAP could only be a perverse numerical coincidence if it did not sug-

gest that the model has physical significance

The approximate equality of  $t_H$  and  $t_v$  for so many particle types suggests that in a fully quantum mechanical theory, the two would indeed be identical. If  $t_H = \hbar/(4mc^2) = t_v$  exactly, then the VAP potential field action  $\mathcal{A} = \frac{1}{2}\hbar$  exactly (compare the definition of  $t_H$  and eqs. (6) and (6')). The near-equalities suggest that the models represent well the dynamics of wave packets in VAPs, just as the Bohr-Sommerfeld quantization represents well the dynamics of electronic wave packets in hydrogen atoms and constituent quarks in mesons<sup>(1)</sup>. Of course quantum mechanics and QFT cannot be equalled by semiclassical methods, but all of these methods have distinguished roles in the understanding of physical problems.

It is quite intriguing that the quantum fluctuation action  $\frac{1}{2}\hbar$  emerges naturally from these model calculations, because source-free considerations of the equations for the electromagnetic field are generally used to obtain the zero-point energy in each wave mode,  $\frac{1}{2}\hbar\omega$ ; in contrast, in the present derivations, the *particles* are the zero-point field sources, as Schwinger showed in QED<sup>(36)</sup>.

It is also interesting that we have been able to let  $R_{int} \rightarrow 0$  in our computations, but it apparently does not make sense for  $R_{int}$  to be smaller than the Planck length  $(\hbar G/c^3)^{1/2} \approx 1.6 \times 10^{-33}$  cm. At this scale, the smoothness of spacetime is thought to break down into a foam-like topology because of quantum gravitational fluctuations<sup>(40)</sup>. This lower limit has no significant effect on the  $t_v$  values because  $R_{max}$  is much greater than the Planck length in every case. (The gravitational force is not amenable to a semiclassical model of the type that has been developed herein, because the VAP models have the symmetry property that antiparticles attract but like particles repel; gravitation is different in that like particles attract as well as antiparticles. If one writes an equation like the energy equation (2) for the gravitational “potential”, then the  $R_{max}$  is less than the Schwarzschild radius of the VAP masses, indicating that the model is not physical )

One possible improvement on this work is to reconstruct the models along the more elaborate lines of Oliver's detailed self-force treatment for the electron<sup>(41)</sup>. However, that would lead to mathematical developments beyond the scope of the present paper. Another approach is to consider how the Dirac two-body equation might be adapted to this problem. Also, in the cases of quark VAPs, it may be that simplified equations for the QCD interactions, which have been studied by Wilczek, could be applicable as alternatives to the Cornell potential; and improve the poor agreement between the model  $t_v$  of the light quark VAPs and their Heisenberg lifetimes.

Because the force constants  $e$  and  $\kappa$  can be expressed in terms of  $\hbar$  and  $c$ , the question arises: why do the electromagnetic and color forces have the strengths that they have? Are other strengths conceivable for these forces in some hypothetical alternative universes, as has been suggested by proponents of the "anthropic principle?"<sup>(42)</sup>

It is risky to generalize from only two instances, but these semiclassical VAP models for electromagnetic and color force interactions have a clear common governing principle: the dynamical VAP timescale must equal the Heisenberg VAP lifetime. We may infer that both the electromagnetic and color force constants take on their respective values because of the  $t_H \approx t_v$  constraints, which imply unique values for  $e$  and  $\alpha_s(q)$ . This suggests that  $\hbar$  and  $c$  are the more fundamental quantities in nature.

This semiclassical modeling method clearly gives correct answers, to good approximation, for the two-body VAPs to which it is applicable. The method therefore deserves to be part of the toolkit for understanding quantum theory of virtual particles.

The author gratefully acknowledges helpful discussions of this work with C. J. Crannell, J. M. Hollis, R. G. Lyon, R. J. Drachman, M. L. Rilee, L. N. Foster, and I. T. Durham. Thanks to J. S. Langton for detecting a computational error in an earlier draft, and for improving the C program used for numerical integration in Sec. 3.3. Constructive recommendations from two referees are also greatly appreciated.

## REFERENCES

1. F. Brau, *Phys. Rev. D* **62**, 014005 (2000).
2. J. J. Sakurai, *Advanced Quantum Mechanics*, Addison-Wesley, Redwood City, Calif. (1967), p. 138; G. C. Wick, *Nature* **142**, 993 (1938); I. J. R. Aitchison, *Contemp. Phys.* **26**(4), 333, in particular p. 369
3. B. Hatfield, *Quantum Field Theory of Point Particles and Strings*, Addison-Wesley, Reading, Mass. (1992), p. 407; P. W. Milonni, *The Quantum Vacuum*, Academic Press, San Diego (1994), Chaps. 9, 10.
4. E. P. Wigner, in *Aspects in Quantum Theory*, ed. A. Salam and E. P. Wigner, Cambridge Univ. Press, London (1972); W. Greiner, in: *Quantum Electrodynamics of Strong Fields*, Plenum, New York (1983), p. 6.
5. R. E. Langer, *Phys. Rev.* **51**, 669 (1938); H. C. von Baeyer, *Phys. Rev. D* **12**(10), 3086 (1975); B. Sheehy and H. C. von Baeyer, *Amer. J. Phys.* **49**(5), 429 (1981).
6. F. Gross, *Relativistic Quantum Mechanics and Field Theory*, Wiley Interscience, New York (1993), p. 337. Also, see R. P. Feynman, in R. P. Feynman and S. Weinberg, *Elementary Particles and the Laws of Physics*, Cambridge Univ. Press, Cambridge (1987), p. 47.
7. F. Gross uses a different diagram convention in which time increases towards the left. Most authors (and Feynman) depict time advancing upward.
8. V. B. Berestetski, E. M. Lifshitz and L. P. Pitaevskii, *Quantum Electrodynamics*, Pergamon Press, Oxford (1982), p. 3.
9. E. C. G. Stückelberg, *Helv. Phys. Acta* **15**, 23 (1942).
10. J. P. Costella, B. H. J. McKellar and A. A. Rawlinson, *Amer. J. Phys.* **65**, 835 (1997).
11. M. A. Trump and W. C. Schieve, *Classical Relativistic Many-Body Dynamics*, Kluwer Acad. Pub., Dordrecht (1999), p. 24.

12. A. Carati, *Foundations of Phys* **28**, 843 (1998).
13. Cf. G. Baym, *Lectures on Quantum Mechanics*, Benjamin, New York (1969), p. 518.
14. J. D. Jackson, *Classical Electrodynamics*, 2nd ed., Wiley, New York (1975), p. 185.
15. J. J. Sakurai, op. cit., p. 140.
16. For a review of positronium theory, see M. A. Stroschio, *Phys. Reps.* **C22**(5), 215 (1975).
17. J. D. Jackson, op. cit., pp. 553-555
18. P. W. Milonni, op. cit., p. 403.
19. E.g., J. Huschilt, W. E. Baylis, D. Leiter, and G. Szamosi, *Phys. Rev. D* **7**(10), 2844 (1973); J. C. Kasher, *J. Phys. A: Math. Gen.* **10**(7), 1097 (1977).
20. J. J. Sakurai, op. cit., p. 118.
21. G. A. Korn and T. M. Korn, *Mathematical Handbook for Scientists and Engineers*, 2nd ed., New York, McGraw-Hill (1968), p. 974.
22. E. M. Purcell, *Electricity and Magnetism* McGraw-Hill, New York (1965), p. 365; J. D. Jackson, op. cit., p. 184.
23. See review by H. C. von Baeyer, *Phys. Rev. D* **12**(10), 3086 (1975); also W. Dittrich and M. Reuter, *Classical and Quantum Dynamics*, Springer-Verlag, Berlin (1994)
24. D. Derbes, *Amer. J. Phys* **64**(7), 881 (1996).
25. C. Lanczos, *The Variational Principles of Mechanics*, 4th ed., Dover, New York (1986), p. 321.
26. F. Gross, op. cit., p. 478.
27. See review by W. Lucha, F. F. Schöberl and D. Gromes, *Phys. Reps.* **200**(4), 127 (1991); in particular, p. 150.
28. D. B. Lichtenberg, *The Standard Model Of Elementary Particles*, Bibliopolis,

- Napoli (1991). pp 128-129.
- 29 S. Bethke, *J. Phys G: Nucl. Part. Phys* **26**, R27 (2000); F. Wilczek, *Phys. Today* **53**(8), 22 (2000).
  30. K. G Chetyrkin, B. A. Kniehl and M. Steinhauser, *Phys. Rev. Lett.* **79**, 2184 (1997).
  31. J. L. Richardson, *Phys. Lett.* **82B**, 272 (1979).
  32. S. Weinberg, *The Quantum Theory of Fields III*, Cambridge Univ. Pres, Cambridge (1996), p. 152.
  33. D. B. Lichtenberg, op. cit., p. 133.
  34. V Fitch, in: *Encycl. of Phys.*, 2nd ed., VCH Publishers, New York (1991), p. 1357; in particular, p. 1360.
  35. K. Rith and A. Schäfer, *Sci. Amer.* **281**, 58 (1999).
  36. See T. Y. Cao, *Conceptual Developments of 20th Century Field Theories*, Cambridge Univ. Press, Cambridge (1998), p. 198; J. Schwinger, *Phys. Rev.* **74**, 1439 (1948); J. Schwinger, *Phys. Rev.* **75**, 651 (1949).
  37. K. Gottfried and V. F Weisskopf, *Concepts of Particle Physics*, Volume II, Oxford Univ Press, New York (1986), p. 263.
  38. B Hatfield, *Quantum Field Theory of Point Particles and Strings*, Addison Wesley, Reading, Mass. (1992), p. 409.
  39. G. Kane, *The Particle Garden*, Addison-Wesley, Reading, Mass. (1995), p. 126.
  40. N. A. Doughty, *Lagrangian Interaction*, Addison Wesley, Reading, Mass. (1990), p 24; J. A. Wheeler, in: *Battelle Rencontres: 1967 Lectures in Mathematics and Physics*, Benjamin, New York (1968), p. 269.
  41. M. A. Oliver, *Foundations Phys.* **11**(1), 61 (1998).
  42. E. g., J. Barrow and F. Tipler, *The Anthropic Principle*, Oxford U. Press, Oxford (1986).

## FIGURE CAPTIONS

Figure 1. (a) Feynman diagram for VEPP life cycle. (Time advances in the upward direction in this figure<sup>(7)</sup>.) The bottom vertex is spacetime point  $x_1$ , the top vertex is spacetime point  $x_2$ . The maximum extent of this process along the time axis is  $t_{He}$ .

(b) Semiclassical VEPP life cycle model. The magnetic moments  $\mu_{e\pm}$  are assumed to point along the axis of separation. The time  $t_2$  corresponds to  $\frac{1}{2}t_{ve}$  in the case of a VEPP.

Figure 2. Magnetic field lines of a positron at the origin. The field is symmetric with respect to rotation about the vertical axis. An example location of a virtual electron is indicated by the vertical arrow, representing its magnetic moment  $\mu_{e-}$ , which must always be parallel with the magnetic moment of the positron because angular momentum is conserved. The dashed lines, which become a pair of cones when rotated about the vertical axis, define the volume where energy conservation permits virtual electrons to exist: within the cones electrons may move, but outside the cones this violates the energy equation (2).



TABLE I.

## Elementary Particles and Their VAP Properties

Particle	Mass (g)	$q/e$	$\alpha_s$	$R_{max}$ (cm) <sup>a</sup>	$t_v$ (s) <sup>a</sup>	$t_H$ (s)
			$\Delta$			
Electron	$9.11 \times 10^{-28}$	-1		$4.7 \times 10^{-12}$	$2.7 \times 10^{-22}$	$3.2 \times 10^{-22}$
Muon	$1.88 \times 10^{-25}$	-1		$2.4 \times 10^{-14}$	$1.3 \times 10^{-24}$	$1.55 \times 10^{-24}$
Tau lepton	$3.16 \times 10^{-24}$	-1		$1.3 \times 10^{-15}$	$7.8 \times 10^{-26}$	$9.23 \times 10^{-26}$
Down quark	$5.9 \times 10^{-25}$	$-\frac{1}{3}$	0.52	$2.1 \times 10^{-14} \textcircled{C}$	$1.4 \times 10^{-24} \textcircled{C}$	
			0.0048	$2.1 \times 10^{-14}$	$1.4 \times 10^{-24}$	$5.0 \times 10^{-25}$
Up quark	$5.9 \times 10^{-25}$	$\frac{2}{3}$	0.52	$2.1 \times 10^{-14} \textcircled{C}$	$1.4 \times 10^{-24} \textcircled{C}$	
			0.0193	$2.1 \times 10^{-14}$	$1.4 \times 10^{-24}$	$5.0 \times 10^{-25}$
Strange quark	$8.9 \times 10^{-25}$	$-\frac{1}{3}$	0.38	$1.0 \times 10^{-14} \textcircled{C}$	$6.7 \times 10^{-25} \textcircled{C}$	
			0.0123	$1.0 \times 10^{-14}$	$6.7 \times 10^{-25}$	$3.3 \times 10^{-25}$
Charm quark	$2.67 \times 10^{-24}$	$\frac{2}{3}$	0.22	$1.9 \times 10^{-15} \textcircled{C}$	$1.3 \times 10^{-25} \textcircled{C}$	
			0.26	$2.3 \times 10^{-15}$	$1.5 \times 10^{-25}$	$1.1 \times 10^{-25}$
Bottom quark	$8.4 \times 10^{-24}$	$-\frac{1}{3}$	0.19	$5.3 \times 10^{-16} \textcircled{C}$	$3.6 \times 10^{-26} \textcircled{C}$	
			0.098	$5.8 \times 10^{-16}$	$3.7 \times 10^{-26}$	$3.5 \times 10^{-26}$
Top quark	$3.1 \times 10^{-22}$	$\frac{2}{3}$	0.11	$8.4 \times 10^{-18} \textcircled{C}$	$5.6 \times 10^{-28} \textcircled{C}$	
			2.0	$1.4 \times 10^{-17}$	$8.6 \times 10^{-28}$	$9.4 \times 10^{-28}$
W boson	$1.42 \times 10^{-22}$	1		$3.0 \times 10^{-17}$	$1.7 \times 10^{-27}$	$2.1 \times 10^{-27}$
Z boson	$1.62 \times 10^{-22}$	0		$2.6 \times 10^{-17}$	$1.5 \times 10^{-27}$	$1.8 \times 10^{-27}$

<sup>a</sup> Two values are given for quarks, the upper number marked with the  $\textcircled{C}$  symbol to indicate that the color-Coulomb potential only was used to derive the value; the lower number is found by including both color-Coulomb and spin-spin potentials.

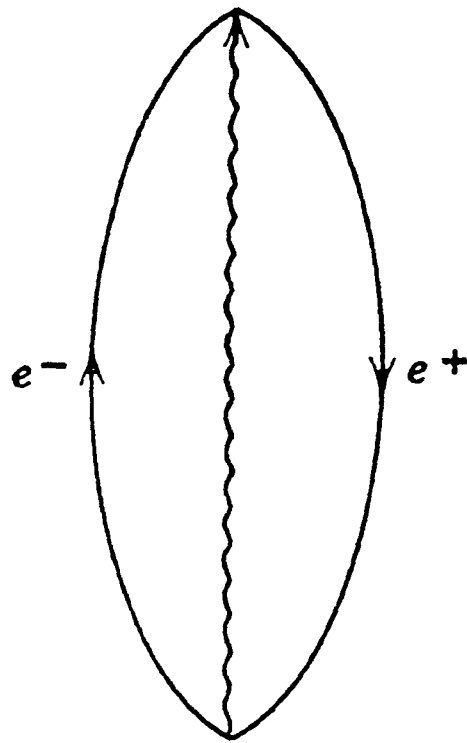


Figure 1(a), The Lifetimes of Virtual  
Antiparticle Pairs I.  
by David Batchelor

Top of figure ↑

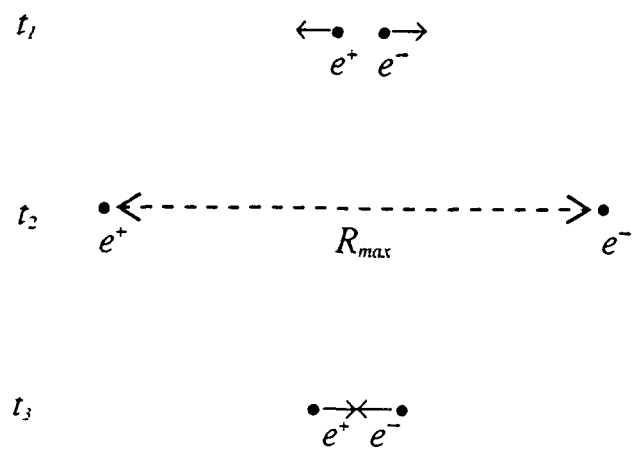


Figure 1(b), The Lifetimes of Virtual Antiparticle Pairs I.  
by David Batchelor

Top of figure ↑

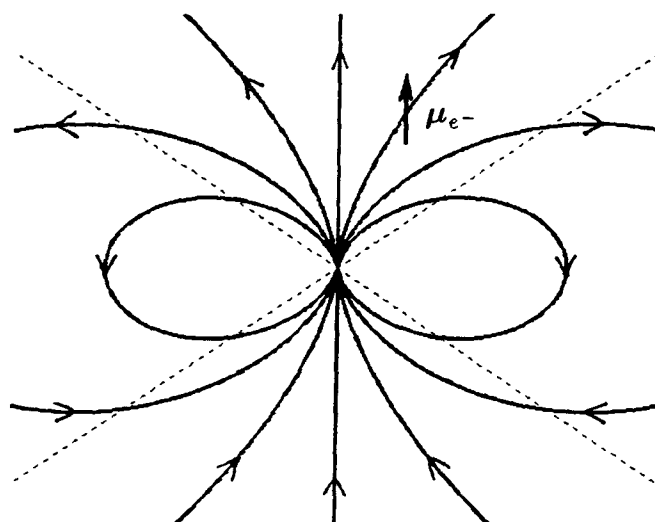


Figure 2, Semiclassical Models for Virtual Antiparticle Pairs, the Unit of Charge  $e$  and the QCD Coupling  $\alpha_s$ , by David Batchelor

Top of figure ↑